Evidence by Electrochemical Impedance Spectroscopy of Surface States Mediated SiMo12O404− Reduction at an n-InP Electrode

ARTICLE *in* THE JOURNAL OF PHYSICAL CHEMISTRY C · OCTOBER 2008

Impact Factor: 4.77 · DOI: 10.1021/jp804899h

2 AUTHORS, INCLUDING:

Catherine Debiemme-Chouvy
Pierre and Marie Curie University - Paris 6
95 PUBLICATIONS **864** CITATIONS

Evidence by Electrochemical Impedance Spectroscopy of Surface States Mediated $SiMo_{12}O_{40}^{4-}$ Reduction at an n-InP Electrode

Catherine Debiemme-Chouvy* and Hubert Cachet

Laboratoire Interfaces et Systèmes Electrochimiques, UPR 15 du CNRS, Université Pierre et Marie Curie, CP 133, 4 Place Jussieu, 75252 Paris Cedex, France

Received: June 3, 2008; Revised Manuscript Received: September 17, 2008

In acidic solution, in the presence of $SiMo_{12}O_{40}^{4-}$, a heteropolyanion, n-InP is spontaneously photoetched. Indeed, under illumination (photon energy >1.35 eV) the polyanions are reduced while the semiconductor undergoes an anodic dissolution process due to the photogenerated holes. It has been established that the reduction of $SiMo_{12}O_{40}^{4-}$ is achieved by electron capture from the InP conduction band. However, one question remained: is the electron capture direct from the InP conduction band or indirect via band gap surface states. In this work, evidence for a two-step mechanism is brought by electrochemical impedance spectroscopy. At the highest tested potentials, the frequency response is dominated by the space-charge capacitance, showing a perfect Mott−Schottky behavior and a flat-band potential of −1.03 V/MSE. For lower potentials, at which cathodic current is flowing, there is evidence for a 70 mV negative band edge shift and a corresponding additional capacitance peak assigned to charge relaxation effects in surface states exchanging electrons both with the InP conduction band and the $SiMo_{12}O_{40}^{4-}$ species present in solution. These states, which are mediators for electron transfer, are located at 0.53 and 0.63 eV with respect to the conduction band minimum.

Introduction

For (opto)electronic device manufacturing, etching of III−V semiconductors is often performed by means of a wet process.[1−3] Wet etching can be carried out, in the dark, either at open circuit potential in the presence of an oxidizing agent or under anodic polarization in an indifferent electrolyte. For n-type semiconductors, localized etching can be achieved using light of energy greater than the material band gap to create electron−hole pairs. Under these conditions, the semiconductor dissolution is obtained under applied potential or in the presence of an oxidizing agent able to pick up some electrons to prevent the occurrence of electron−hole recombination. This ensures that some photogenerated holes are available to trigger the semiconductor dissolution.

For a better control of the etching process, it is essential to know the reaction mechanism and then the relevant experimental parameters. Recently, it was shown that n-InP could be selectively, with respect to p-InP, photoetched under open circuit conditions using an unusual oxidizing agent, namely, the dodecamolybdosilicate Keggin-type heteropolyanion (HPA), α-$SiMo_{12}O_{40}^{4-}$.[4,5] This compound (noted $SiMo_{12}$) is able to capture a large number of electrons compensated, in acidic solution, by a protonation process.

At an n-InP electrode, in 0.5 M H_2SO_4 solution, for potentials between −0.25 and −0.65 V/MSE the reduction of $SiMo_{12}$ takes place according to the following reaction:[6]

$$SiMo^{VI}{}_{12}O_{40}^{4-} + 2e^- + 2H^+ \rightarrow H_2SiMo^{VI}{}_{10}Mo^{V}{}_2O_{40}^{4-} \quad (1)$$

Moreover, this process is diffusion-limited and irreversible.[6] On the contrary, at a metallic electrode such as platinum electrode, in a potential range of 0 to −0.6 V/MSE, the voltammogram of $SiMo_{12}$ exhibits three reversible redox waves at potentials of −0.18, −0.3, and −0.48 V/MSE (see Figure 1).[7]

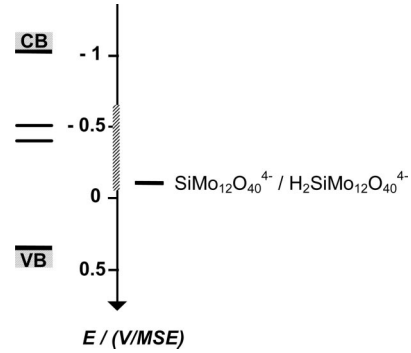

Figure 1. Energy level diagram showing the first redox standard potential of $SiMo_{12}$ (ref 7) with respect to the band edge positions of InP (VB, valence band; CB, conduction band), at pH = 0.3. The dashed potential range corresponds to the potentials explored in the present work. Both lines shown in the band gap correspond to the surface states determined here.

For the most oxidized $SiMo_{12}$ form, all the Mo atoms are in the +VI oxidation state. Reduction of HPA occurs by successive steps, the oxidation state of a number of Mo atoms being reduced at +V (blue HPA).[8]

As previously demonstrated,[5,6] dissolution of n-InP immersed in a $SiMo_{12}$ acidic solution is observed under visible light illumination, in electroless conditions. Actually, under illumination electron−hole pairs are photogenerated, some electrons are captured by $SiMo_{12}$ avoiding the electron−hole recombination, and therefore some holes are available for the corrosion of n-InP. In the dark, no dissolution occurs allowing for a localized photoetching of the semiconductor.

It has been evidenced that the electrochemical reduction of $SiMo_{12}$ at an n-InP surface involves the semiconductor conduction band.[6] However, the remaining question was the charge

* Corresponding author. E-mail: catherine.debiemme-chouvy@upmc.fr. Tel.: 33 1 44 27 41 49. Fax: 33 1 44 27 40 74.

10.1021/jp804899h CCC: $40.75
Published on Web 10/28/2008

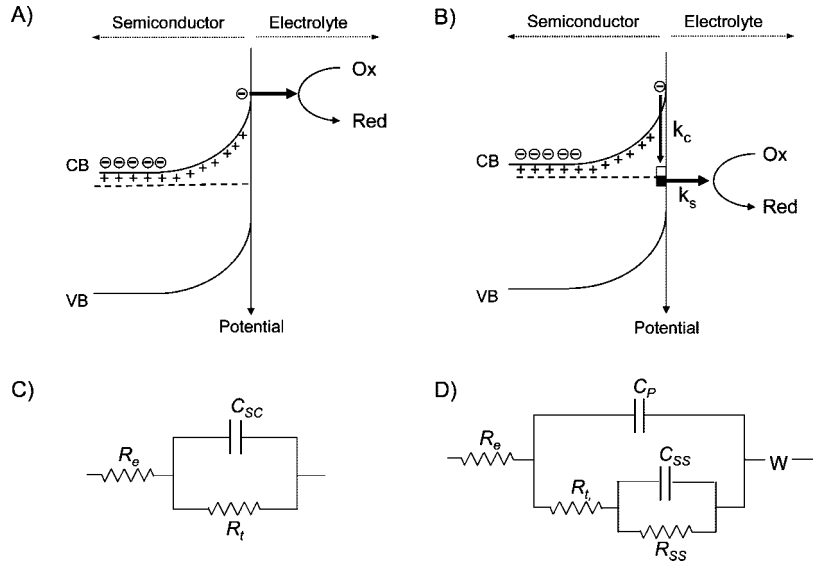

Figure 2. (A and B) Scheme of charge-transfer mechanisms at an n-type semiconductor electrode during reduction of a species in solution by electron capture (A) from the conduction band or (B) from surface states. (C and D) electrical equivalent circuits corresponding to mechanism A and B, respectively. C_P is either C_{SC} or $C_{SC} + C_{SS}$*.

transfer to be direct from the conduction band (Figure 2A) or indirect, via localized band gap surface states (Figure 2B).[9−13] As justified in the following, at pH = 0.3, the flat-band potential V_{fb} of n-InP lies at −1.03 V/MSE. As a consequence, the first redox level of $SiMo_{12}$ is much more positive (0.85 eV) than the n-InP conduction band minimum at the surface (see Figure 1). Therefore, electron transfer from the n-InP conduction band to $SiMo_{12}$ is likely to be mediated by surface states (S) according to the formal reactions (Figure 2B)

$$e^-_{CB} + S \rightarrow S^- \quad (2)$$

$$2S^- + SiMo_{12}O_{40}{}^{4-} + 2H^+ \rightarrow 2S + H_2SiMo_{12}O_{40}{}^{4-} \quad (3)$$

Such a mechanism was proposed by Tyagai and Kolbasov to account for the Fe^{3+} and $Fe(CN)_6{}^{3-}$ reduction at n-CdS and n-CdSe electrodes,[14] by Hens and Gomes for Fe^{3+} reduction at n-GaAs electrode,[15] and by Parthasarathy et al. for $Fe(CN)_6{}^{3-}$ reaction at ZnO multipod.[16]

In order to specify the electron-transfer mechanism from n-InP to $SiMo_{12}$, electrochemical impedance spectroscopy (EIS) measurements were performed. The involvement of surface states in $SiMo_{12}$ reduction process is pointed out through band edge shift and the existence of an excess capacitance peak, in agreement with a kinetic modeling of electron exchanges between the surface states, the InP conduction band, and the $SiMo_{12}$ redox species.

Experimental Methods

All the experiments were performed with single-crystal tin-doped (100) n-InP electrodes supplied by MCP Electronic Materials Ltd. (U.K.). The carrier concentration was close to $N_d = 10^{18}$ cm^{-3}. The silicomolybdic acid, α-$H_4SiMo_{12}O_{40}$, was purchased from Aldrich. After nitrogen bubbling, deaerated aqueous solutions of 10^{-3} M α-$H_4SiMo_{12}O_{40}$ in 0.5 M H_2SO_4 were used, maintained under inert atmosphere. Electrochemical measurements were carried out in a three-electrode cell under potentiostatic control (Solartron 1287 potentiostat) at room temperature and in the dark. The n-InP surface area was 0.25 cm^2. The counter electrode was a platinum grid, and the reference electrode was a mercurous sulfate electrode (MSE). A Solartron 1260 transfer function analyzer coupled to a Solartron 1287 potentiostat was used for impedance measurements in the frequency range of 0.1 Hz to 60 kHz using Fracom software. Impedance diagrams were analyzed by comparison to equivalent electrical circuits using ZsimpWin software from PAR.

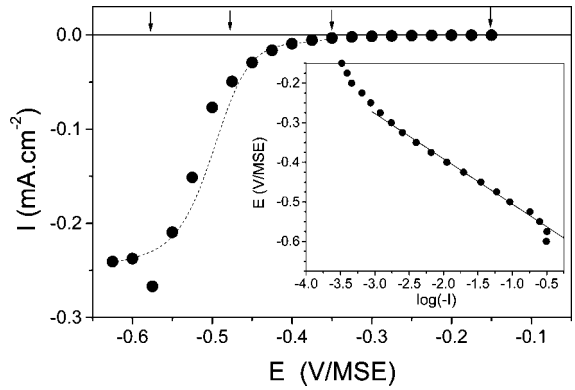

Figure 3. Steady-state voltamperogram obtained at an n-InP electrode in 10^{-3} M $SiMo_{12}$ + 0.5 M H_2SO_4 solution (currents measured during EIS experiments). Dashed line: curve calculated according to eq 5. Inset: representation in logarithm scale. The impedance diagrams obtained at the potentials indicated by an arrow are shown in Figure 4.

Results

Impedance spectra and the stationary current were simultaneously recorded from −0.15 to −0.625 V/MSE by step of 25 mV, in the dark. The current density−potential curve obtained under stationary conditions is depicted in Figure 3. The current is due to the reduction of the first system of $SiMo_{12}$ (eq 1). When plotted in a logarithmic scale, a linear part is observed between −0.3 and −0.5 V/MSE with a slope 114 mV per decade of current.

Note that after impedance measurement at potential at which HPA reduction occurs, the electrode open circuit potential (OCP) is lower than the initial one. This observation is explained by the fact that in the electrolyte only the oxidized form of $SiMo_{12}$ is present. After cathodic polarization, the concentration of the reduced form at the electrode/solution interface has increased; thus, the OCP is lower (Nernst equation). Progressively, the

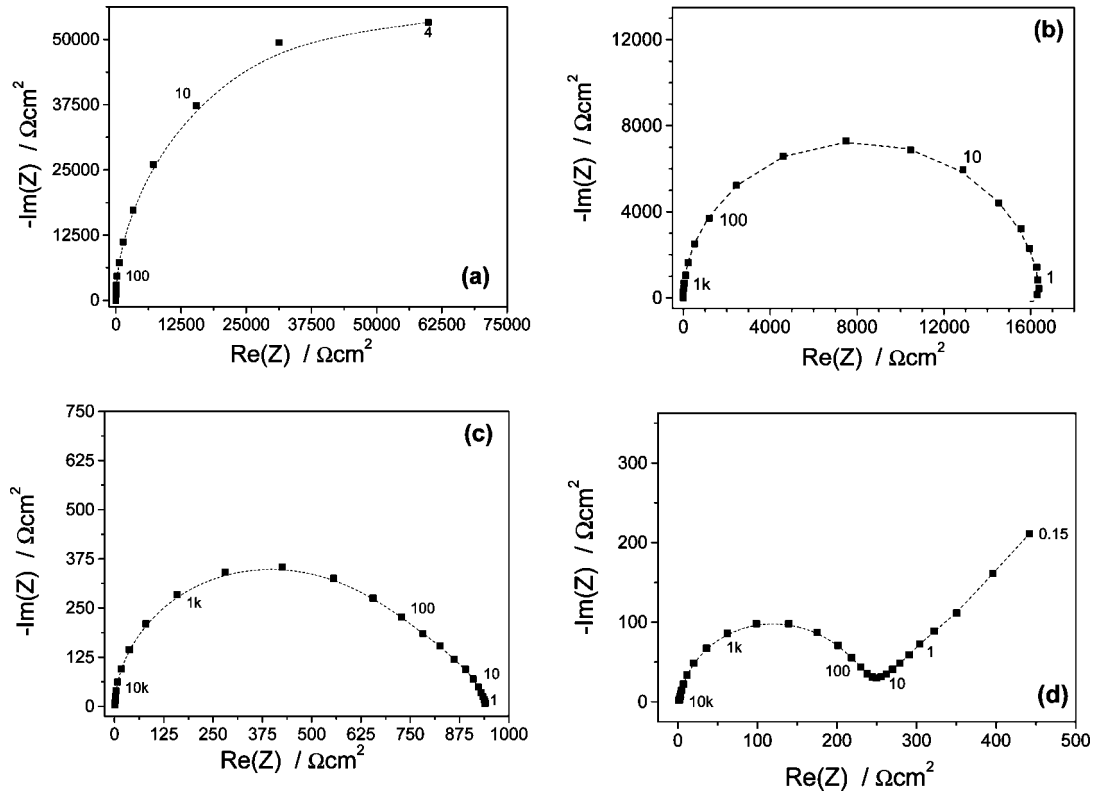

Figure 4. Impedance spectra recorded at (a) −0.15, (b) −0.35, (c) −0.475, and (d) −0.575 V/MSE, for n-InP in contact with 10^{-3} M $SiMo_{12}$ + 0.5 M H_2SO_4 solution. Squares: experimental data. Dotted lines: calculated data according to the equivalent circuit shown in Figure 2D. The fitting parameters are reported in Table 1. $R_e = 1.5\ \Omega\cdot cm^2$.

TABLE 1: Values of the Parameters Used to Fit the Experimental Impedance Spectra Obtained by Polarization of an n-InP Electrode in the Presence of 10^{-3} M $SiMo_{12}$[a]

E (V/MSE)	C_p ($nF\cdot cm^{-2}$)[b]	R_t ($\Omega\cdot cm^2$)	R_{ss} ($\Omega\cdot cm^2$)	C_{ss} ($\mu F\cdot cm^{-2}$)	W_0 ($\Omega\cdot cm^2\cdot s^{0.5}$)
−0.15[c]	351	109 900	21 900	6.40	
−0.175	346	176 500	133 000	0.17	
−0.2	351	169 800	95 300	0.24	
−0.225	358	177 100	40 630	15.2	
−0.25	361	85 700	30 980	0.46	
−0.275	368	53 200	18 020	0.77	
−0.3	372	35 800	10 300	1.30	
−0.325	377	23 700	5820	1.90	
−0.35[c]	382	13 100	3290	2.70	
−0.375	385	7270	1880	3.31	
−0.4	394	4020	1010	4.74	
−0.425	398	2280	639	5.31	
−0.45	408	1260	399	6.50	
−0.475[c]	414	704	221	10.3	
−0.5	418	413	119	7.00	
−0.525	444	216	55	4.82	70.5
−0.55	622	181	81	2.32	37.7
−0.575[c]	1090	133	91	2.49	71

[a] The electrical equivalent circuit is shown in Figure 2D. [b] C_p corresponds to either C_{SC} or $C_{SC} + C_{SS}$*. [c] Simulated spectra are shown in Figure 4 (dashed lines).

reduced species diffuse into the electrolyte bulk leading to an increase of the OCP until reaching its initial value.[6]

Parts a−c of Figure 4 show the Nyquist diagrams obtained in the low current potential range ($-0.15 \geq E > -0.5$ V/MSE).

A classical Randles circuit[17] (Figure 2C), as expected in the case of a direct electron transfer between the semiconductor conduction band and a redox species in solution (Figure 2A), did not allow us to simulate our experimental impedance data. The existence of a distribution of time constants suggests us considering a transfer mechanism via surface states (Figure 2B) since it has been shown that the $SiMo_{12}$ reduction occurs by electron capture (and not by hole injection into the valence band).[6] In fact, two time constants were used to well account for our impedance data, leading to the electrical equivalent circuit given in Figure 2D. This circuit is similar to the one used for n-GaAs/Fe^{3+} system.[15] It is the most simple that can be considered for an indirect charge transfer. It is composed of the electrolyte resistance R_e ($\approx 1.5\ \Omega\cdot cm^2$) in series with a circuit involving the n-InP space-charge capacitance C_{sc} (or C_p) in parallel with a transfer resistance R_t in series with a parallel resistance−capacitance (R_{ss}, C_{ss}) circuit (Figure 2D). Thus, the capacitive loop involves two time constants, R_tC_p and $R_{ss}C_{ss}$. With this model, the electronic transfer is frequency-dependent, due to the involvement of surface states. With the increase of the cathodic current, the presence of the second time constant in the Nyquist diagram becomes more visible (Figure 4, parts b and c). At large current densities, there is an additional contribution due to mass transport accounted for by a Warburg element $W_0(j\omega)^{-0.5}$ in series with the previously described electrical equivalent circuit (Figure 4d). It is remarkable that no constant phase element (CPE) was required as expected for a single-crystal semiconductor with low surface roughness immersed in a highly conductive electrolyte.[18]

The values of the fitted parameters corresponding to the electrical equivalent circuits previously described and depicted in Figure 2D are listed in Table 1. From the calculated confidence intervals, the relative error on C_{sc} is 1−2% but is much larger for C_{ss} as exemplified in Figure 5. In this figure, the values of C_{ss} versus potential are depicted with their error bars. In spite of the limited precision, a capacitance peak is clearly observed at −0.48 V/MSE with a shoulder located around −0.4 V/MSE. C_{ss} can be assigned to surface states responsible for the band edge shift observed in the Mott−Schottky

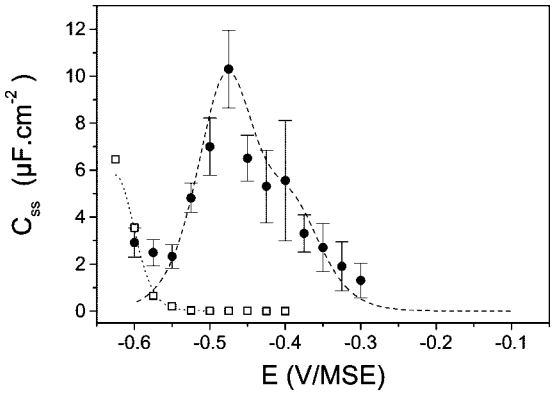

Figure 5. Dependence on potential of the surface state capacitance C_{ss} (full circles) and C_{ss}* (open squares). Dotted curves: simulated data according to eqs 8 and 11.

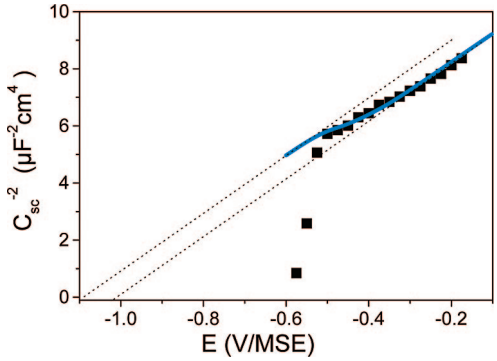

Figure 6. Mott−Schottky plot for the n-InP/$SiMo_{12}$ system. Squares correspond to the data obtained from the impedance spectra. Full line: data calculated according to eq 10.

plot (Figure 6) and presumed playing a role in the electron transfer between InP and the $SiMo_{12}$ species.

Figure 6 shows the potential dependence of C_{sc} in the Mott−Schottky representation. At the most positive potentials, over 200 mV, a linear variation is obtained, yielding an extrapolated flat-band potential E_{fb} of −1.03 V/MSE, in very good agreement with the literature.[19,20] From the slope, a donor density N_d equals to 1.1×10^{18} cm^{-3} is found, in agreement with the supplier specifications. At potentials lower than −0.3 V/MSE, potentials at which $SiMo_{12}$ reduction occurs (see Figure 3), there is a systematic deviation from linearity, pointing out a progressive band edge shift toward negative potentials. Its amplitude reaches about 70 mV. This shift that is potential-dependent is ascribed to surface state charging. Note that X-ray photoelectron spectroscopy (XPS) analyses performed after $SiMo_{12}$ reduction have shown that no species are adsorbed on the InP surface.[4]

At potentials more negative than −0.5 V/MSE, there is a large increase in the so-called C_p capacitance in the equivalent circuit analysis (Figure 2D). It means that an additional capacitance C_{ss}* lies in parallel with the space-charge capacitance C_{sc}. C_{ss}* can be evaluated by subtracting the actual value of C_{sc} calculated by extrapolating the Mott−Schottky plot linearly, from the total capacitance C_p. The relative error on C_{ss}* is about 2%. The values are plotted in Figure 5 (open squares). C_{ss}* can be interpreted as the signature of a distribution of additional states in the vicinity of the conduction band minimum, only yielding to surface charge effects, with an energy-distributed state density, 1 or 2 orders of magnitude lower than that of the two localized states identified above.

Discussion

In this section, it will be shown that the current−voltage response of the n-InP/$SiMo_{12}$ interface can be quantitatively accounted for by considering the contribution of localized surface states superimposed to that of the InP space-charge capacitance. These discrete surface states exchange electrons with the semiconductor conduction band and with the electroactive species in solution. These states allow the cathodic current due to $SiMo_{12}$ species reduction to start at potentials largely positive with respect to the flat-band potential but at lower potential than at a metallic electrode (see Figure 1). At an applied potential E, the cathodic current $I(E)$ flowing through surface states can be written for one state

$$I(E) = qk_s N_{ss} f_{ss} c_{HPA} \tag{4}$$

or for a distribution of states

$$I(E) = qk_s c_{HPA} \int_{\Delta E_g} N_{ss}(E_g) f_{ss}(E_g)\, dE_g \tag{5}$$

where N_{ss} is the surface state density and f_{ss} is the fill factor of the state at energy E_{ss} with respect to the InP conduction band. k_s is the rate constant for electron capture by HPA species whose concentration is c_{HPA}; q is the elementary charge; E_g is the energy position within the band gap relative to the conduction band minimum. The integral is taken over the energy domain ΔE_g corresponding to the state distribution. Filling of surface states is calculated using the Hall−Schockley−Read statistics[21] with the two conditions: (i) experiments are performed in the dark, and (ii) the state distribution is located in the upper part of the InP band gap. The contribution of holes can then be neglected. The surface state capacitance C_{ss} is defined by the following expression:

$$C_{ss}(E) = \frac{q^2}{kT} \int_{\Delta E_g} N_{ss}(E_g) \frac{df_{ss}}{dV_{sc}}\, dE_g \tag{6}$$

where V_{sc} is the potential seen by the semiconductor, which differs from the applied potential E because of the surface charge effects. k and T have their usual meaning. A small variation dE of E is distributed through the interface as

$$dE = dV_{sc} + dV_H \tag{7}$$

dV_{sc} is the change in band bending and dV_H = dQ_{ss}/C_H is the elementary potential change across the Helmholtz layer at the electrolyte side of the interface due to a change dQ_{ss} of the surface charge. The full expression of $C_{ss}(E)$ is then

$$C_{ss}(E) = \frac{q^2}{kT} \int_{\Delta E_g} \frac{N_{ss}(E_g) k_c^2 n_s n_1}{[k_s c_{HPA} + k_c(n_s + n_1)]^2}\, dE_g \tag{8}$$

n_s, the surface electron density in the conduction band, and n_1 are expressed as

$$n_s(E) = N_d \exp\left[\frac{q(E_{fb} + \Delta V_H(E) - E)}{kT}\right] \text{ and } n_1(E_{ss}) = N_c \exp\left(\frac{-E_{ss}}{kT}\right) \tag{9}$$

where E_{fb} is the flat-band potential, N_c is the effective density of states in the conduction band (for InP, $N_c = 5.6\ 10^{17}$ cm^{-3} [22]), and $\Delta V_H(E) = Q_{ss}(E)/C_H$ is the actual potential drop in the Helmholtz layer calculated by integrating the surface state charge $Q_{ss}(E)$ from a potential value for which $C_{ss} = 0$ (i.e., −0.1 V) to the considered E value. Accordingly the potential dependence of the space-charge capacitance C_{sc} is written as

$$C_{sc}^{-2}(E) = \frac{2}{q\varepsilon\varepsilon_0 N_d}[E - (E_{fb} + \Delta V_H(E))] \quad (10)$$

where ε is the static dielectric permittivity of InP ($\varepsilon = 12.4$) and $\varepsilon_0 = 8.84 \times 10^{-12}$ F m^{-1}.

On the basis of this model, the experimental results for $C_{ss}(E)$ and $C_p(E)$ (Figures 6 and 5, respectively, and Table 1) were quantitatively simulated by assuming two localized states with a Gaussian energy distribution of the form

$$N_{ss}(E_g) = N_t \exp\{-0.5[(E_g - E_p)/\sigma]^2\} \quad (11)$$

where N_t is the surface state density at the peak energy, E_p, referred to the conduction band minimum, and σ is related to the curve width. The parameters obtained for the two surface states are, respectively, $N_t = 5.1 \times 10^{11}$ cm^{-2} (1.3×10^{11} cm^{-2}), $E_p = 0.535$ eV (0.630 eV), and $\sigma = 0.005$ eV (0.01 eV). Therefore, the density of surface states interacting with $SiMo_{12}$ species is equal to 10^{10} cm^{-2}.

The surface state distributions found in the present work are hardly comparable to literature data. However, recently, Saraf et al. studied the local energy distribution of surface state density within InP band gap using Kelvin probe force microscopy.[23] The method was applied to measure the contact potential difference of a cross-sectional pn junction grown by molecular beam epitaxy under different environments, vacuum or nitrogen atmosphere. For a p^{++}n-InP(110) surface junction, a donor state was identified at 0.66 eV ($N_t = 8.1 \times 10^{11}$ cm^{-2}) or 0.735 eV ($N_t = 3.8 \times 10^{12}$ cm^{-2}) below the conduction band minimum in vacuum or under nitrogen, respectively. Moreover, Ahaitouf et al. studied the nonideality of (100) n-InP/Au Schottky diodes. They reported on a continuous state distribution at the upper half of the band gap of InP with a peak surface states density of 4.5×10^{12} cm^{-2} eV^{-1} located at 0.56 eV below the conduction band minimum.[24]

Note that, in a review paper on the formation of semiconductor interfaces, Flores and Tejedor indicate that the cation dangling bond level for InP was calculated to be 0.53 eV with respect to the conduction band minimum.[25] The latter finding is close to the state location found from our electrochemical experiments, suggesting that the states involved in the mediation of electron transfer between InP and $SiMo_{12}$ species would be indium-related states.

The negative charge stored in these states when scanning from positive to negative potentials, and the corresponding band edge shift ($\approx$ 70 mV), is able to reproduce the nonlinearity depicted by the Mott−Schottky plot in Figure 6. This good agreement was obtained by taking $C_H = 20$ μF cm^{-2}, thus providing a direct evaluation of the Helmholtz capacitance at the n-InP/H_2SO_4 solution interface.

According to the present model, the interfacial current flowing through the surface states reproduces the experimental current−voltage curve in all the potential range explored, validating a state-mediated electron-transfer mechanism (dashed line, Figure 3). The corresponding values for the rate constants are $k_c = 6 \times 10^{-7}$ cm^3 s^{-1} and $k_s = 5 \times 10^{-18}$ cm^3 s^{-1}. At the most negative potentials, the model predicts a current limitation due to the localized character of the surface states involved, as shown by experiments, too. Because of a possible contribution of diffusion, not taken into account by the model, the rate constant k_s could be slightly underestimated.

Finally, the distribution of surface states in the band gap of InP, as deduced from a detailed analysis of impedance data of an n-InP/$SiMo_{12}$ junction, is summarized in Figure 7. It is shown that in the 0.4−0.7 eV range below the conduction band minimum, the main contribution is that of the two localized states at 0.535 and 0.63 eV which could act as mediators for the electrochemical reduction of $SiMo_{12}$ species, the other states being electrochemically inactive.

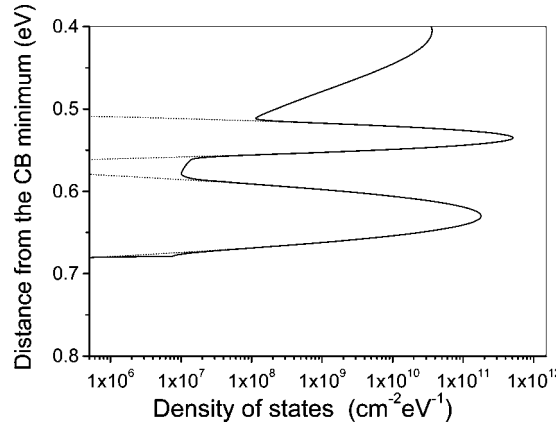

Figure 7. Energy location inside the band gap of InP vs surface state density, deduced from the impedance data.

Conclusions

The n-InP/H_2SO_4 interface in the presence of $SiMo_{12}$ was characterized by EIS in a potential range in which $SiMo_{12}$ species are reduced. Impedance analyses show that in addition to the InP space-charge capacitance a potential-dependent excess capacitance existed. The latter is interpreted as the signature of surface states acting as mediators for $SiMo_{12}$ reduction. The experimental data, dc current and capacitive responses, were simulated by considering two localized surface states with a Gaussian energy distribution and peaking at 0.535 and 0.63 eV below the InP conduction band minimum. According to literature, they are probably indium-related states.

As a more general comment, this study shows that energy distribution of surface states can be quantitatively determined in an electrochemical way by combining impedance analysis of a semiconductor/electrolyte junction in the presence of adequately chosen redox species.

References and Notes

(1) Notten, P. H. L.; Van den Meerakker, J. E. A. M.; Kelly, J. J. *Etching of III−V Semiconductors. An Electrochemical Approach*; Elsevier Advanced Technology: Oxford, U.K., 1991.
(2) Clawson, A. R. *Mater. Sci. Eng.* **2001**, *R 31*, 1.
(3) Gomes, W. P. Wet etching of III−V semiconductors In *Handbook of Advanced Electronic and Photonic Materials and Devices*; Nalwa, H. S., Ed.; Academic Press: San Diego, CA, 2001.
(4) Quennoy, A.; Rothschild, A.; Gerard, I.; Etcheberry, A.; Debiemme-Chouvy, C. *J. Cluster Sci.* **2002**, *13*, 313.
(5) Debiemme-Chouvy, C.; Quennoy, A.; Gérard, I. *Electrochem. Commun.* **2002**, *4*, 97.
(6) Debiemme-Chouvy, C.; Quennoy, A. *Electrochim. Acta* **2004**, *49*, 3129.
(7) Launay, J. P.; Massart, R.; Souchay, P. *J. Less-Common Met.* **1974**, *36*, 139.
(8) Pope, M. T. *Heteropoly and Isopoly Oxometalates*; Springer: Heidelberg, Germany, 1983.
(9) Gerischer, H. *J. Phys. Chem.* **1991**, *95*, 1356.
(10) Vanmaekelbergh, D. *Electrochim. Acta* **1997**, *42*, 1121.
(11) Fajardo, A. M.; Lewis, N. S. *J. Phys. Chem. B* **1997**, *101*, 11136.
(12) Hens, Z. *J. Phys. Chem. B* **1999**, *103*, 122.
(13) Gomes, W. P.; Vanmaekelbergh, D. *Electrochim. Acta* **1996**, *41*, 967.
(14) Tyagai, V. A.; Kolbasov, G. Y. *Surf. Sci.* **1971**, *28*, 423.

(15) Hens, Z.; Gomes, W. P. *J. Phys. Chem. B* **1999**, *103*, 130.
(16) Parthasarathy, M.; Ramgir, N. S.; Sathe, B. R.; Mulla, I. S.; Pillai, V. K. *J. Phys. Chem. C* **2007**, *111*, 13092.
(17) Bard, A. J.; Faulkner, L. R. *Electrochemical Methods: Fundamental and Applications*, 2nd ed.; John Wiley and Sons: New York, 2001.
(18) Oskam, G.; Vanmaekelbergh, D.; Kelly, J. J. *J. Electroanal. Chem.* **1991**, *315*, 65.
(19) Tubbesing, K.; Meissner, D.; Memming, R.; Kastening, B. *J. Electroanal. Chem.* **1986**, *214*, 685.
(20) Iranzo-marin, F.; Debiemme-Chouvy, C.; Herlem, M.; Sculfort, J.-L.; Etcheberry, A. *J. Electroanal. Chem.* **1994**, *365*, 283.
(21) Allongue, P.; Cachet, H. *J. Electrochem. Soc.* **1985**, *132*, 45.
(22) *Semiconductors. Group IV Elements and III−V Compounds, Data in Science and Technology*; Madelung, O., Ed.; Springer-Verlag: Berlin, Germany, 1991.
(23) Saraf, S.; Schwarzman, A.; Dvash, Y.; Cohen, S.; Ritter, D.; Rosenwaks, Y. *Phys. Rev. B* **2006**, *73*, 035336–1.
(24) Ahaitouf, A.; Bath, A.; Losson, E.; Abarkan, E. *Mater. Sci. Eng., B* **1998**, *52*, 208.
(25) Flores, F.; Tejedor, C. *J. Phys. C: Solid State Phys.* **1987**, *20*, 145.

JP804899H